EFFECT OF INDUCED MAGNETIC FIELD ON NON-NEWTONIAN NANOFLUID Al_2O_3 MOTION THROUGH BOUNDARY-LAYER WITH GYROTACTIC MICROORGANISMS

by

Nabil T. ELDABE*, Raafat R. RIZKALLA, Mohamed Y. ABOU-ZEID, and Vivian M. AYAD

Department of Mathematics, Faculty of Education,
Ain Shams University, Roxy, Cairo, Egypt

Original scientific paper
https://doi.org/10.2298/TSCI200408189E

The effect of the induced magnetic field on the motion of Eyring-Powell nanofluid Al_2O_3, containing gyrotactic microorganisms through the boundary-layer is investigated. The viscoelastic dissipation is taken into consideration. The system is stressed by an external magnetic field. The continuity, momentum, induced magnetic field, temperature, concentration, and microorganisms equations that describe our problem are written in the form of 2-D non-linear differential equations. The system of non-linear PDE is transformed into ODE using appropriate similarity transformations with suitable boundary conditions and solved numerically by applying the NDSolve command in the MATHEMATICA program. The obtained numerical results for velocity, induced magnetic field, temperature, the nanoparticles concentration, and microorganisms are discussed and presented graphically through some figures. The physical parameters of the problem play an important role in the control of the obtained solutions. Moreover, it is obvious that as Grashof numbe increases, both the velocity, f', and the induced magnetic field, h', increase, while, the reciprocal magnetic Prandtl number, A, works on decreasing both f' and h'. As Eckert number increases the temperature increases, while it decreases as the velocity ratio B increases.

Key words: *boundary-layer, non-Newtonian nanofluid, induced magnetic field, microorganisms*

Introduction

The boundary-layer problem is the most important advanced study in fluid mechanics. Boundary-layers may be either laminar or turbulent depending on the value of Reynolds number. Khan *et al.* [1] studied the problem of laminar boundary-layer flow of a nanofluid past a stretching sheet. They analyzed the effects of both Brownian motion and thermophoresis. Bachok *et al.* [2] investigated the problem of the boundary-layer of nanofluid-flow over a moving semi-infinite flat plate, the flat plate is supposed to move in the same or opposite directions to the free stream. The problem of boundary-layer flow of a nanofluid past a stretching sheet under the effects of Brownian motion and thermophoresis is studied analytically by Hassani *et al.* [3], it is found that the solution of the problem depends on the Brownian motion number, thermophoresis number, Prandtl number, and Lewis number. Many researchers [4-6] studied the boundary-layer flow of a nanofluid past a vertical plate. Nield *et al.* [7] examined analyti-

* Corresponding author, e-mail: eldabe_math@yahoo.com

cally the problem of natural-convection past a vertical plate in a porous medium saturated by a nanofluid. Furthermore, the MHD boundary-layer flow with heat and mass transfer of nanofluids over a non-linearly stretching sheet with the effect of viscous dissipation is analyzed numerically by Mabood *et al.* [8]. Abou-Zeid [9] studied the MHD boundary-layer heat transfer in the laminar boundary-layer flow with viscous dissipation and heat generation in a porous medium.

The study of non-Newtonian fluids has attracted attention in recent years because of the use of many applications in different fields such as industry and engineering. The different types of non-Newtonian fluids are explained by many researchers [10-16]. Bhatti *et al*. [17] invitegated the flow of Jeffrey fluid with small suspended particles through tapered duct with compliant walls in the presence of magnetic field, the fluid is electrically conducting, incompressible, irrotational with constant density. the peristaltic motion of non-Newtonian fluid with heat and mass transfer under the effect of a magnetic field through a porous medium is discussed by Eldabe *et al*. [18]. Zhang *et al*. [19] discussed the entropy analysis of prestaltic blood flow through an anisotropically tapered arteries with suspened magnetic ZnO. The blood is considered to obey Jeffrey fluid model under the effect of magnetic field. The problem of peristaltic flow of non-Newtonian blood fluid with heat and mass transfer through a non-uniform channel is studied by Eldabe *et al*. [20]. Eldabe *et al*. [21] also studied the problem of boundary-layer flow of MHD non-Newtonian nanofluid with heat and mass transfer under the effect of radiation, heat generation, and chemical reaction through a porous medium. Furthermore, the solution of the boundary-layer flow of an Eyring Powell fluid over a linearly stretching sheet is studied by Rahimi [22].

Nanofluids are fluids containing nanometer-sized particles. Nanofluids are mixtures of base fluid and nanoparticles. The nanoparticles used in nanofluids are made of metals, oxides, carbides or carbon nanotubes. Common base fluids include water, ethylene glycol, and oil. The problem of boundary-layer stagnation-point flow of nanofluid past a stretching sheet with an induced magnetic field is studied by Gireesha *et al.* [23]. Sheikholeslami and Rokni [24] investigated the two-phase nanofluid double diffusion convection in the existence of an induced magnetic field. The influence of the induced magnetic field on free convection of nanofluid is analyzed by Sheikholeslami *et al.* [25]. The effect of the induced magnetic field on peristaltic flow was examined by many researchers [26-28]. The MHD flow of non-Newtonian Eyring Powell nanofluid over a non-linear stretching sheet is investigated by Hayat *et al.* [29]. Eldabe *et al.* [30] discussed the problem of a 2-D boundary-layer flow of MHD non-Newtonian nanofluid through a porous medium. The problem of MHD peristaltic flow with heat tranfer of non-Newtonian biviscosity nanofluid in eccentric annuli is discussed by Abou-Zeid [31]. Ali *et al.* [32] studied the problem of MHD stagnation-point flow over a stretching sheet under the effect of the induced magnetic field. Recently, many researchers [33-36] have discussed the nanofluid-flow containing gyrotactic microorganisms. Zaffar and Iqbal [37] discussed the interaction of induced magnetic field and stagnation-point flow on bioconvection nanofluid containing gyrotactic microorganisms. Furthermore, the simultaneous effects of coagulation and variable magnetic field on the peristaltic induced motion of Jeffrey nanofluid containing gyrotactic microorganisms is illustrated by Bhatti *et al.* [38], the effect of endoscope is taken as special case.

The main aim of this study is to investigate the effect of the induced magnetic field on the motion of non-Newtonian nanofluid Al_2O_3, through the boundary-layer containing gyrotactic microorganisms. After applying the similarity transformations of the system of the governing equations, these equations are transformed to non-linear ODE which have been solved numerically using MATHEMATICA 9. The effects of different parameters on these transformed equations have been discussed and presented graphically. Physically, our model can be applied to gyrotactic microorganisms with an endo-scope.

Mathematical formulation

We consider a 2-D boundary-layer flow with the effect of the induced magnetic field on the motion of non-Newtonian nanofluid in the presence of gyrotactic microorganisms. The stress tensor for the non-Newtonian Eyring Powell model [13]:

$$\tau_{ij} = \mu\frac{\partial u_i}{\partial x_j} + \frac{1}{\beta}\sinh^{-1}\left(\frac{1}{c}\frac{\partial u_i}{\partial x_j}\right) \tag{1}$$

where μ is the dynamic viscosity and β and c are the material fluid parameters. Considering:

$$\sinh^{-1}\left(\frac{1}{c}\frac{\partial u_i}{\partial x_j}\right) \cong \frac{1}{c}\frac{\partial u_i}{\partial x_j} - \frac{1}{6}\left(\frac{1}{c}\frac{\partial u_i}{\partial x_j}\right)^3, \quad \left|\frac{1}{c}\frac{\partial u_i}{\partial x_j}\right| \ll 1 \tag{2}$$

We assumed that the x-axis is along the sheet and y-axis is normal to the sheet as shown in fig. 1. The magnetic Reynolds number is assumed to be large. It is also supposed that a uniform magnetic field of strength, H_0, acts in the y-direction while the normal component of the induced magnetic field H_2 vanishes when it reaches the wall and the parallel component, H_1, approches the value of H_0 [39]. The temperature, concentration, and microorganisms at the wall are denoted as T_w, C_w and n_w, respectively. Also, the values of T, C, and n as y tends to infinity are denoted by T_∞, C_∞, and n_∞, respectively. The velocity at the wall is given by $u_w = ax$ and the free stream velocity is given by $u_\infty = bx$, where a and b are positive constants.

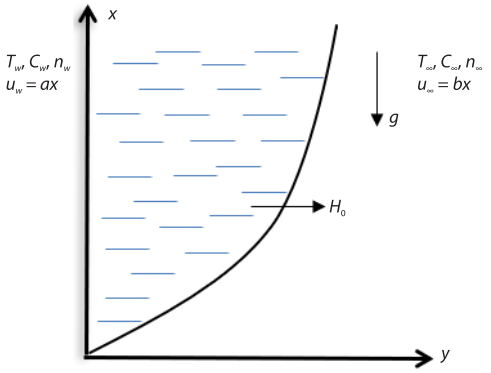

Figure 1. The physical model of the problem

Under these assumptions, the governing boundary-layer equations of non-Newtonian nanofluid with thermophoretic diffusion as well as Maxwell equations can be written:

$$\frac{\partial u}{\partial x} + \frac{\partial v}{\partial y} = 0 \tag{3}$$

$$\frac{\partial H_1}{\partial x} + \frac{\partial H_2}{\partial y} = 0 \tag{4}$$

$$u\frac{\partial u}{\partial x} + v\frac{\partial u}{\partial y} = \frac{1}{\rho_f}\left(\mu + \frac{1}{\beta c}\right)\frac{\partial^2 u}{\partial y^2} - \frac{1}{\rho_f \beta c^3}\left(\frac{\partial u}{\partial y}\right)^2\left(\frac{\partial^2 u}{\partial y^2}\right) + \\ + \frac{\mu_e}{\rho_f}\left(H_1\frac{\partial H_1}{\partial x} + H_2\frac{\partial H_1}{\partial y}\right) - \frac{1}{2\rho_f}\mu_e H_e\frac{\partial H_e}{\partial x} + \\ + \frac{1}{\rho_f}\left[\left(1-C_\infty\right)\rho_f \mathrm{g}\beta_T\left(T-T_\infty\right) - \left(\rho_p - \rho_f\right)\mathrm{g}\left(C-C_\infty\right) - \mathrm{g}\gamma'\left(\rho_m - \rho_f\right)\left(n-n_\infty\right)\right] \tag{5}$$

$$H_1\frac{\partial u}{\partial x} + H_2\frac{\partial u}{\partial y} = u\frac{\partial H_1}{\partial x} + v\frac{\partial H_1}{\partial y} - \frac{1}{\mu_e\sigma}\frac{\partial^2 H_1}{\partial y^2} \tag{6}$$

$$u\frac{\partial T}{\partial x}+v\frac{\partial T}{\partial y}=\frac{k}{\left(\rho c_p\right)_f}\left(\frac{\partial^2 T}{\partial y^2}\right)+\frac{\left(\rho c_p\right)_p}{\left(\rho c_p\right)_f}\left\{D_B\left(\frac{\partial C}{\partial y}\frac{\partial T}{\partial y}\right)+\frac{D_T}{T_\infty}\left(\frac{\partial T}{\partial y}\right)^2\right\}+$$
$$+\frac{1}{\left(\rho c_p\right)_f}\left(\mu+\frac{1}{\beta c}\right)\left(\frac{\partial u}{\partial y}\right)^2-\frac{1}{6\left(\rho c_p\right)_f\beta c^3}\left(\frac{\partial u}{\partial y}\right)^4 \tag{7}$$

$$u\frac{\partial C}{\partial x}+v\frac{\partial C}{\partial y}=D_B\frac{\partial^2 C}{\partial y^2}+\frac{D_T}{T_\infty}\frac{\partial^2 T}{\partial y^2} \tag{8}$$

$$u\frac{\partial n}{\partial x}+v\frac{\partial n}{\partial y}+\frac{bW_c}{\left(C-C_\infty\right)}\left[\frac{\partial n}{\partial y}\frac{\partial C}{\partial y}+n\frac{\partial^2 C}{\partial y^2}\right]=D_n\frac{\partial^2 n}{\partial y^2} \tag{9}$$

where u and v are the velocity components in the x-and y-directions Also H_1 and H_2 are the magnetic components in the x- and y-directions.

The subjected boundary conditions are:

$$\begin{gathered}u=u_w=ax,\ v=0,\ \frac{\partial H_1}{\partial y}=H_2=0,\ T=T_w,\ C=C_w,\ n=n_w,\ \text{at}\ \ y=0\\ u\to u_\infty=bx,\ v=0,\ H_1=H_e\left(x\right)\to H_0\left(x\right),\ T\to T_\infty,\ C\to C_\infty\\ n\to n_\infty,\ \text{as}\ \ y\to\infty\end{gathered} \tag{10}$$

Introducing the similarity transformations:

$$\begin{gathered}\eta=y\sqrt{\frac{a}{\nu}},\ \psi=\sqrt{a\nu}xf\left(\eta\right),\ H_1=H_0xh'\left(\eta\right),\ H_2=-H_0\sqrt{\frac{\nu}{a}}h\left(\eta\right)\\ \theta\left(\eta\right)=\frac{T-T_\infty}{T_w-T_\infty},\ \phi\left(\eta\right)=\frac{C-C_\infty}{C_w-C_\infty},\ \chi\left(\eta\right)=\frac{n-n_\infty}{n_w-n_\infty}\end{gathered} \tag{11}$$

where

$$u=\frac{\partial\psi}{\partial y},\ v=-\frac{\partial\psi}{\partial x}$$

in which ψ is the stream function.

The system of eqs. (5)-(9) can be transformed to:

$$\left(1+\epsilon\right)f'''-\epsilon\delta f''^2\ f'''-f'^2+ff''+M\left(h'^2-hh''-1\right)+\mathrm{Gr}\left(\theta-Nr\phi-Rb\chi\right)=0 \tag{12}$$

$$Ah'''+fh''-f''h=0 \tag{13}$$

$$\theta''+\mathrm{Pr}f\theta'+Nb\phi'\theta'+Nt\theta'^2+\mathrm{Ec}\epsilon f''^2+\frac{\mathrm{Ec}\epsilon\delta}{3}f''^4=0 \tag{14}$$

$$\phi''+\mathrm{PrLe}f\phi'+\frac{Nt}{Nb}\theta''=0 \tag{15}$$

$$\chi''+Lbf\chi'-\mathrm{Pe}\left[\phi'\chi'+\phi'\left(\Omega+\chi\right)\right]=0 \tag{16}$$

With the boundary conditions:

$$f(0)=1,\ f'(0)=1,\ h(0)=h''(0)=0,\ \theta(0)=1,\ \phi(0)=1$$
$$\chi(0)=1,\ \text{at}\ \eta=0 \tag{17}$$
$$f'(\infty)\to B,\ h'(\infty)\to 1,\ \theta(\infty)\to 0,\ \phi(\infty)\to 0,\ \chi(\infty)\to 0,\ \text{as}\ \eta\to\infty$$

Where the dimensionless parameters are:

$$\epsilon=\frac{1}{\mu\beta c},\ \delta=\frac{a^3x^2}{2\nu c^2},\ M=\frac{\mu_e H_0^2}{4\pi\rho_f a^2},\ \mathrm{Gr}=\frac{g\beta_T(1-C_\infty)(T-T_\infty)}{a^2x},\ \mathrm{Ec}=\frac{a^2x^2}{c_p\alpha(T-T_\infty)},\ B=\frac{b}{a}$$
$$Nr=\frac{(\rho_p-\rho_f)(C_w-C_\infty)}{\beta_T\rho_f(1-C_\infty)(T-T_\infty)},\ \mathrm{Rb}=\frac{\gamma'(n_w-n_\infty)(\rho_m-\rho_f)}{\beta_T\rho_f(1-C_\infty)(T-T_\infty)} \tag{18}$$
$$\mathrm{Pr}=\frac{\nu_f}{\alpha},\ Nb=\frac{\tau D_B(C_w-C_\infty)}{\alpha},\ \mathrm{Lb}=\frac{\nu_f}{D_n},\ \mathrm{Le}=\frac{\nu_f}{D_B},\ \Omega=\frac{n_\infty}{n_w-n_\infty}$$
$$Nt=\frac{\tau D_T(T_w-T_\infty)}{\alpha T_\infty},\ \mathrm{Pe}=\frac{bW_c}{D_n},\ A=\frac{\mu_e}{\nu}$$

where ϵ and δ are non-Newtonian fluid parameters, M – the magnetic parameter, Gr – the Grashof number, Ec – the modified Eckert number, B – the velocity ratio, Nr – the buoyancy ratio parameter, Rb – the bioconvection Rayleigh number, Pr – the Prandtl number, Nb – the Brownian motion parameter, Lb – the bioconvection Lewis number, Le – the standard Lewis number, Ω – the microorganisms concentration difference parameter, Nt – the thermophoresis parameter, Pe – the bioconvection Peclet number, and A – the reciprocal magnetic Prandtl number.

Numerical results and discussion

The systems of non-linear differential eqs. (12)-(16) subjected to the boundary conditions (17) are solved numerically by applying NDSolve command in MATHEMATICA package v. 9, which apply shooting method and requires the supply of starting values of the missing initial and terminal conditions. Then, we use Rung-Kutta-Merson method with variable step size in order to control the local truncation error, then it applies modified Newton-Raphson technique mentioned before to make successive corrections to the estimated boundary values. The process is repeated iteratively until convergence is obtained *i.e.* until the absolute values of the difference between every two successive approximations of the missing conditions is less than ε (in our case ε is taken = 10^{-6}).

The effects of different parameters on the dimensionless velocity, induced magnetic field, temperature, concentration, and microorganisms are discussed and presented graphically through some figures. The dimensionless velocity, induced magnetic field, temperature, the concentration of nanoparticles, and microorganisms are discussed and presented graphically under the effects of various physical parameters through the figs. 2-17.

The effects of magnetic parameter, M, velocity ratio, B, the reciprocal magnetic Prandtl number, A, non-Newtonian parameter, ϵ, bioconvection Ralyieh number, Rb, buoyancy ratio parameter, Nr, microorganisms concentration parameter, Ω, modified Eckert number, and other parameters on velocity f', respectively, are stated in figs. 2-5. In fig. 2, the velocity f' increases with an increase in the magnetic parameter, M. Figure 3 illustrates the effect of the Grashof number on the velocity f', it is found that as the Grashof number increases the velocity f' slightly increases. Also, the effect of other parameters such as the Brownian motion param-

eter, *Nb*, microorganisms concentration, Ω , the modified Eckert number on the velocity f' are discussed, they are work on slightly increase the velocity f'. But these graphs are excluded to preserve the space of the paper. In fig. 4, the velocity f' decreases with an increase in the reciprocal magnetic Prandtl number, A. Also, the velocity f' slightly decreases under the effects of the non-Newtonian parameter, ϵ, the buoyancy ratio parameter, Nr, and the bioconvection Rayleigh number, Rb. These graphs are also not included. The effect of the velocity ratio parameter, B, on the velocity f' is shown in fig. 5, it is found that the velocity f' decreases with an increase of the B in the interval [0, 4), while it increases by increasing the B in the interval (4, 5].

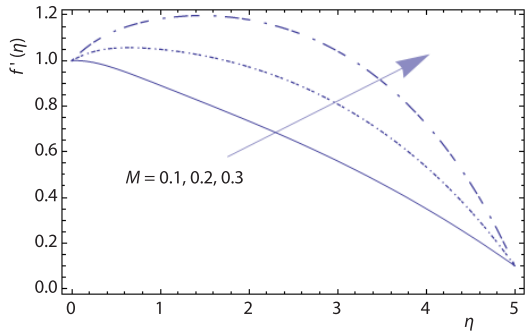

Figure 2. Velocity f' for different values of M with ϵ = Lb = 5, $\delta = \Omega$ = 0.5, Gr = 4, $Nr = Nb = Nt = B$ = 0.1, Rb = 0.2, A =2, Pr = 6.2, Ec = $\gamma = \lambda$ = Pe = 1, Le = 3

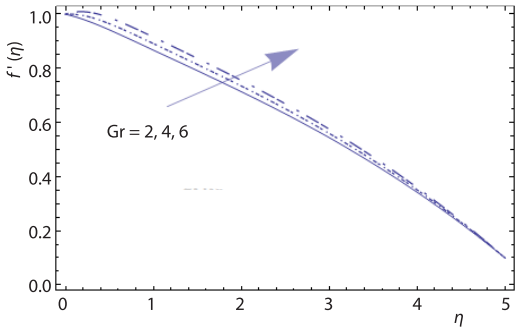

Figure 3. Velocity f' for different values of Gr with ϵ = Lb = 5, $\delta = \Omega$ = 0.5, $M = Nr = Nb = Nt = B$ = 0.1, Rb = 0.2, A = 2, Pr = 6.2, Ec = $\gamma = \lambda$ = Pe = 1, Le = 3

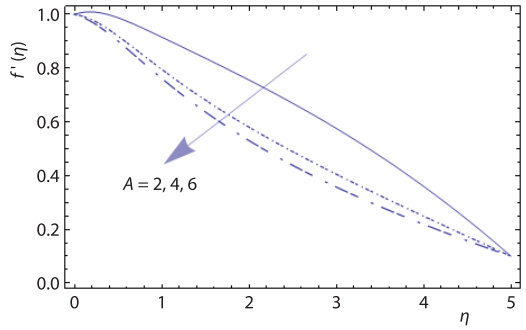

Figure 4. Velocity f' for different values of A with ϵ = Lb = 5, $\delta = \Omega$ = 0.5, Gr = 6, $Nr = M = Nb = Nt = B$ = 0.1, Rb = 0.2, Pr = 6.2, Ec = $\gamma = \lambda$ = Pe = 1, Le = 3

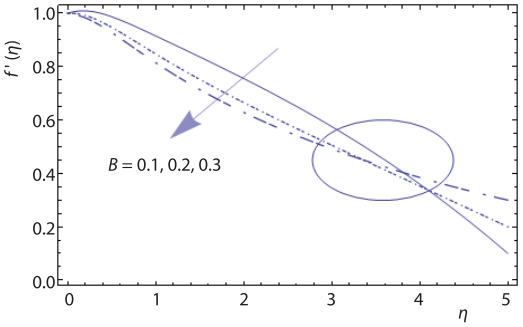

Figure 5. Velocity f' for different values of B with ϵ = Lb = 5, $\delta = \Omega$ = 0.5, Gr = 6, $Nr = Nt = M$ = 0.1, Rb = 0.2, A = 2, Pr = 6.2, Ec = $\gamma = \lambda$ = Pe = 1, Le = 3

The effects of the M, Grashof number, Prandtl number, ϵ, Nr, bioconvection Raylieh number, Eckert number, the modified fluid parameter, γ, and Ω , on the induced magnetic field h', respectively, are illustrated through figs 6-8. In fig. 6, the h' increases with an increase in the Grashof number. It also increases with the increase of the Ω. The effect of the modified Eckert number and γ on the h' are work on slightly increases the h' and these graphs are excluded. Figure 7, illustrates the effect of the reciprocal magnetic Prandtl number on the h', it is found that the h' decreases with an increase in the values of magnetic Prandtl number. The velocity ratio B works on decreasing the h' as well. Other parameters such as the ϵ, bioconvection Raylieh number, and the Nr also works on slightly decreasing the h', but these figures are excluded. In fig. 8, the h' decreases with an increase in the M in the interval [0,1.8), while it increases with an increase in the M in the interval (1.8, 5].

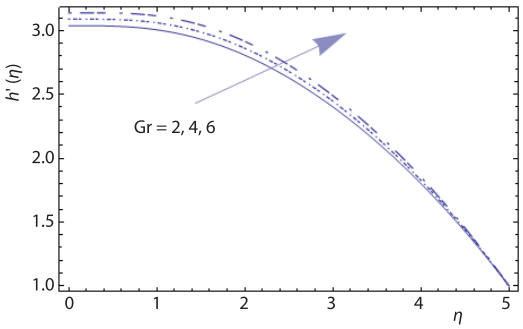

Figure 6. Induced magentic field h' for different values of Gr with ϵ = Lb = 5, $\delta = \Omega = 0.5$, $A = 2$, $Nr = M = Nb = Nt = B = 0.1$, Rb = 0.2, Pr = 6.2, Ec = $\gamma = \lambda$ = Pe = 1, Le = 3

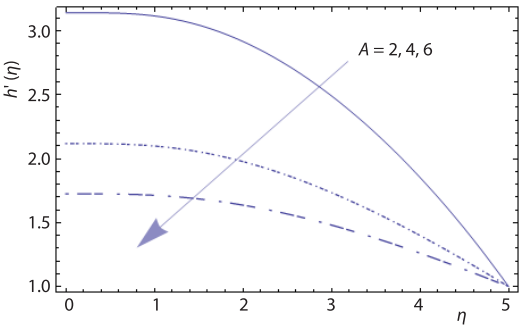

Figure 7. Induced magentic field h' for different values of A with ϵ = Lb = 5, $\delta = \Omega = 0.5$, Gr = 6, $Nr = M = B = Nb = Nt = 0.1$, Rb = 0.2, Pr = 6.2, Ec = $\gamma = \lambda$ = Pe = 1, Le = 3

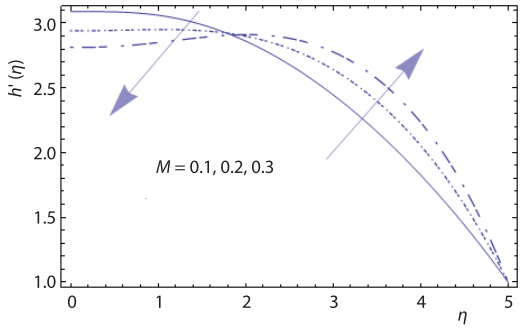

Figure 8. Induced magentic field h' for different values of M with Le = 3, ϵ = Lb = 5, $\delta = \Omega = 0.5$, $A = 2$, $Nr = B = Nb = Nt = 0.1$, Rb = 0.2, Gr = 4, Pr = 6.2, Ec = $\gamma = \lambda$ = Pe = 1

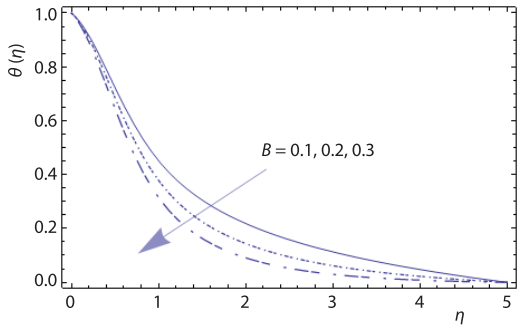

Figure 9. Temperature θ for different values of B with ϵ = Lb = $A = \gamma$ = 5, $\delta = \Omega = 0.5$, $Nr = M = Nb = Nt = 0.1$, Rb = 0.2, Pr = 6.2, Ec = 7, Le = 3, Pe = λ, Gr = 1

Figures 9-11, illustrate the effects of the B, Eckert number, Grashof number, M, magnetic Prandt number, γ, and on the temperature, θ, respectively. Figure 9, shows the effect of the B, on the θ, as the B increases the θ decreases. In fig. 10, the θ increases with an increase in the values of the Eckert number. Also, the θ increases with an increase in the γ, but this figure

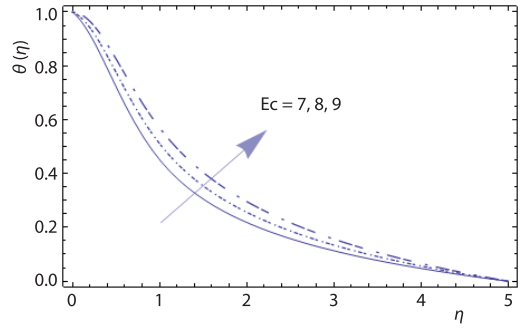

Figure 10. Temperature θ for different values of Ec with ϵ = Lb = $A = \gamma$ = 5, $\delta = \Omega = 0.5$, $Nr = M = Nb = Nt = B = 0.1$, Rb = 0.2, Pr = 6.2, Le = 3, Pe = Gr = λ = 1

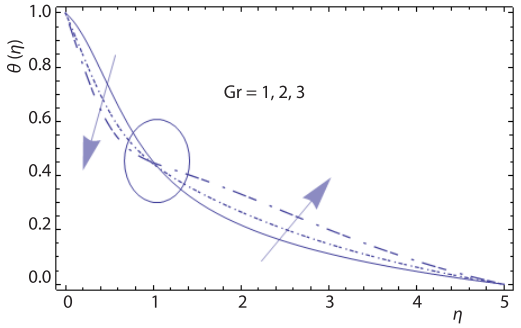

Figure 11. Temperature θ for different values of Gr with ϵ = Lb = $A = \gamma$ = 5, $\delta = \Omega = 0.5$, $Nr = B = M = Nb = Nt = 0.1$, Rb = 0.2, Pr = 6.2, Ec = 7, Le = 3, Pe = λ = 1

is excluded. In fig. 11, the θ decrease with an increase in the Grashof number in the interval [0, 1), while it increases with an increase in the Grashof number in the interval (1, 5]. Also, the θ decreases with an increase in the M in the interval [0, 1.8), while it increases with an increase in the M in the interval (1.8, 5] and this figure is excluded.

The effects of the Lewis number, Nt, B, Eckert number, γ, Nb, magnetic Prandtl number, Nr, and M, on the concentration of nanoparticles, ϕ, respectively, are discussed through the figs. 12 and 13. Figure 12, illustrates the effect of the Lewis number on the ϕ, it is found that the ϕ decreases with an increase in the Lewis number. Also, the ϕ decreases with an increase of other parameters such as the M and Nb. It also slightly decreases with an increase in the modified fluid parameter and the Eckert number. But these figures are excluded to maintain the design of the research. In fig. 13, the ϕ increases with an increase in the Nt. Also, the effect of the Nr on the ϕ is analyzed, it works on increasing the ϕ. The effects of other parameters like the reciprocal magnetic Prandtl number and B on the ϕ are explained, it is found that the ϕ slightly increases under the effect of these parameters. Also, these figures are excluded.

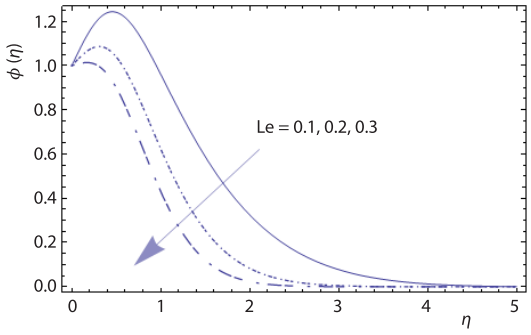

Figure 12. Concentration ϕ for different values of Le with ϵ = Lb = 5, $\delta = \Omega = 0.5$, $A = 2$, $Nr = M = Nb = Nt = B = 0.1$, Rb = 0.2, Pr = 6.2, Ec = $\gamma = \lambda$ = Pe = 1, Gr = 6

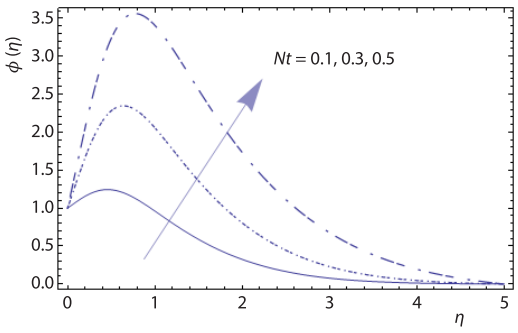

Figure 13. Concentration ϕ for different values of Nt with ϵ = Lb = 5, $\delta = \Omega = 0.5$, $A = 2$, $Nr = M = Nb$ = Le = B = 0.1, Rb = 0.2, Pr = 6.2, Ec = $\gamma = \lambda$ = Pe = 1, Gr = 6

The effect of the bioconvection Lewis number, bioconvection Peclet number, Ω, Nt, B, Eckert number, Nb, magnetic Prandtl number, bioconvection Rayleigh number, Nr, Grashof number, and M on the χ, respectively, are illustrated through the figs. 14-17. In fig. 14, the χ increases with an increase in the bioconvection Lewis number. It also increases with an increase in other parameters such as the reciprocal magnetic Prandtl number, and the bioconvection Rayleigh number. But these figures are excluded. In fig. 15, the χ decreases with an increase in the bioconvection Peclet number. Also, the effects of other parameters such as the Eckert and Lewis numbers, Nr, Grashof number, and the M on the χ are discussed, they are work on decreasing the χ. But these figures also are excluded. Figure 16, illustrates the effect of the Ω on the χ, it is found that the χ increases with an increase in the Ω in the interval [0, 1.2), while it decreases with an increase in the Ω in the interval (1.2, 5]. Also, χ increases with an increase in the the B in the interval [0, 1.8), while it decreases with an increase in the B in the interval (1.8, 5]. Other parameter such as the Nb works on increasing the χ in the interval [0, 1.4), and works on decreasing the χ in the interval (1.4, 5]. But these figures are also excluded. In fig. 17, the χ decreases with an increase in the Nt in the interval [0, 1.6) and it increases with an increase in the Nt in the interval (1.6, 5].

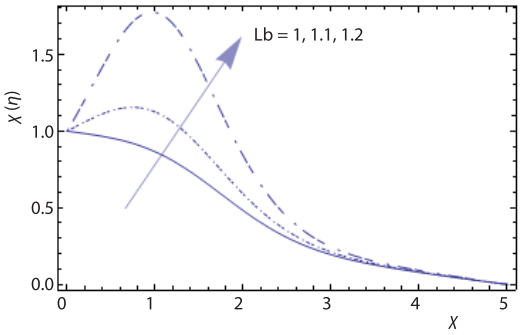

Figure 14. Microorganisms χ for different values of Lb with ϵ = Le = 5, δ = 0.5, $A = Nr = Nb = Nt = B$ = Pe = 0.1, Rb = 0.2, Pr = 6.2, Ec = $\gamma = \lambda = \Omega$ = Gr = 1

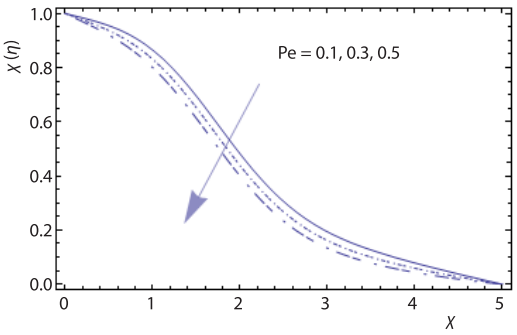

Figure 15. Microorganisms χ for different values of Pe with ϵ = Le = 5, δ = 0.5, $A = Nr = Nb = Nt = B$ = 0.1, Rb = 0.2, Pr = 6.2, Ec = $\gamma = \lambda$ = Lb = $M = \Omega$ = Gr = 1

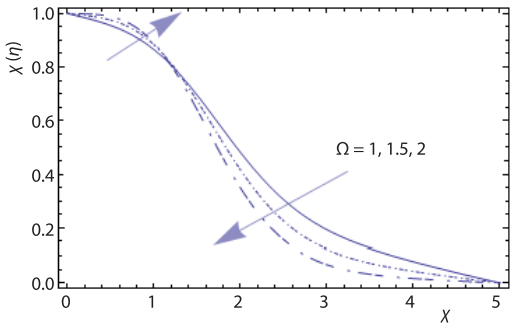

Figure 16. Microorganisms χ for different values of Ω with ϵ = Le = 5, δ = 0.5, $A = Nr = Nb = Nt = B$ = Pe = 0.1, Rb = 0.2, Pr = 6.2, M = Ec = $\gamma = \lambda$ = Lb = Gr = 1

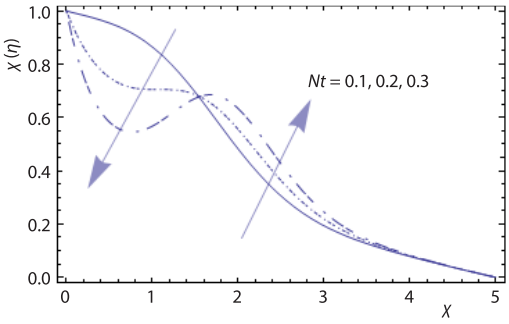

Figure 17. Microorganisms χ for different values of Nt with ϵ = Le = 5, δ = 0.5, $A = Nr = Nb = Nt = B$ = Pe = 0.1, Rb = 0.2, Pr = 6.2, M = Ec = $\gamma = \lambda = \Omega$ = Gr = 6

Conclusions

The problem of the boundary-layer of non-Newtonian nanofluid with gyrotactic microorganisms under the effect of an induced magnetic field has been solved numerically and the graphs are obtained by using MATHEMATICA. The effects of different parameters on the velocity, induced magnetic field, temperature, concentration, and microorganisms are illustrated. This study has many applications to novel microbial fuel cell technologies Sensors and Biosensors. The following results are summarized as follows.

- The f' increases with an increase in the M and the Grashof number. While it decreases with an increase in the reciprocal magnetic Prandtl number.
- The h' increases with an increase in the Grashof number. While it decreases with an increase in the reciprocal magnetic Prandtl number. Furthermore, it decreases with an increase in the M in the interval [0, 1.8), while it increases in the interval (1.8, 5].
- The θ increases with an increase in the Eckert number. While it decreases with an increase in the B. Furthermore, it decreases with an increase in the Grashof number in the interval [0, 1), while it increases in the interval (1, 5].
- The ϕ increases with an increase in the Nt. While it decreases with an increase in the standard Lewis number.

- The χ increase with an increase in the bioconvection Lewis number. While it decreases with an increase in the Peclet number. Furthermore, it increases in the Ω in the interval [0, 1.2), while it decreases in the interval (1.2, 5]. In addition, the χ decreases with an increase in the Nt in the interval [0, 1.4), while it increases in the interval (1.4, 5].

Compliance with ethical standards

Funding information is not applicable /No funding was received.

Conflict of interest

The authors declare that they have no conflict of interest.

Nomenclature

a, b – constant of chemotaxis
C – nanoparticle volume fraction, [molm^{-3}]
C_∞ – ambient nanofluid volume fraction, [molm^{-3}]
C_w – wall nanofluid volume fraction, [molm^{-3}]
c – fluid parameter
c_p – specific heat capacity, [Jkg^{-1}K^{-1}]
D_B – Brownian diffusion coefficient, [m^{2}s^{-1}]
D_n – diffusivity coefficient of microorganisms, [m^{2}s^{-1}]
D_T – thermophoretic diffusion coefficient, [m^{2}s^{-1}]
f' – dimensionless velocity
g – gravitational acceleration, [ms^{-2}]
H_0 – uniform magnetic field, [Tesla]
H_e – magnetic field at the edge, [Tesla]
h' – dimensionless induced magnetic field
k – thermal conductivity, [Wm^{-1}K^{-1}]
n – concentration of microorganisms, [molm^{-3}]
n_∞ – ambient concentration of microorganisms, [molm^{-3}]
n_w – wall concentration of microorganisms, [molm^{-3}]
T – temperature, [K]
T_∞ – ambient temperature, [K]
T_w – wall temperature, [K]
W_c – maximum speed of microorganisms, [ms^{-1}]
x – distance along the surface, [m]
y – distance normal to the surface, [m]

Greek symbols

α – thermal diffusivity of nanofluid, [m^{2}s^{-1}]
β, γ – fluid parameters
γ' – microorganisms average volume fraction, [molm^{-3}]
β_T – thermal expansion coefficient, [K^{-1}]
ϵ, δ – non-Newtonian fluid parameters
η – similarity variable
θ – dimensionless temperature
μ – dynamic viscosity, [kgm^{-1}s^{-1}]
χ – dimensionless microorganisms
ν_f – kinematics viscosity of nanofluid, [ms^{-1}]
ρ_f – fluid density, [kgm^{-3}]
ρ_p – nanoparticle mass density, [kgm^{-3}]
σ – electric conductivity, [sm^{-1}]
τ – ratio of heat capacity of nanoparticle and base fluid
τ_{ij} – stress tensor
ϕ – dimensionless nanoparticle volume fraction
ψ – stream function, [ms^{-2}]
Ω – microorganismus concentration parameter

References

[1] Khan, W. A., aPop, I., Boundary-Layer Flow of a Nanofluid Past a Stretching Sheet', *Int. J. Heat Mass Transf.*, *53* (2010), 11-12, pp. 2477-2483
[2] Bachok, N., *et al.*, Boundary-Layer Flow of Nanofluids over a Moving Surface in a Flowing Fluid, *Int. J. Therm. Sci.*, *49* (2010), 9, pp. 1663-1668
[3] Hassani, M., *et al.*, An Analytical Solution for Boundary-Layer Flow of a Nanofluid Past a Stretching Sheet, *Int. J. Therm. Sci.*, *50* (2011), 11, pp. 2256-2263
[4] Ouaf, M. E., Abou-Zeid, M. Y., Electromagnetic and Non-Darcian Effects on a Micropolar Non-Newtonian Fluid Boundary-Layer Flow with Heat and Mass Transfer, *Int. J. Appl. Electromagn. Mech.*, *66* (2021), 4, pp. 693-703
[5] Eldabe, N. T. M., *et al.*, Thermal Diffusion and Diffusion Thermo Effects of Eyring – Powell Nanofluid-Flow with Gyrotactic Microorganisms through the Boundary-Layer, Heat Transfer – *Asian Res.*, *49* (2020), 1, pp. 383-405
[6] Kuznetsov, A. V., Nield, D. A., Natural Convective Boundary-Layer Flow of a Nanofluid Past a Vertical Plate: A Revised Model, *Int. J. Therm. Sci.*, *77* (2014), Mar., pp. 126-129

[7] Nield, D. A., Kuznetsov, A. V., The Cheng-Minkowycz Problem for the Double-Diffusive Natural Convective Boundary-Layer Flow in a Porous Medium Saturated by a Nanofluid, *Int. J. Heat Mass Transf., 54* (2011), 1-3, pp. 374-378
[8] Mabood, F., *et al*., The MHD Boundary-Layer Flow and Heat Transfer of Nanofluids over a Non-Linear Stretching Sheet: A Numerical study, *Journal Magn. Magn. Mater*., *374* (2015), Jan., pp. 569-576
[9] Abou-Zeid, M. Y., Magnetohydrodynamic Boundary-Layer Heat Transfer to a Stretching Sheet Including Viscous Dissipation and Internal Heat Generation in a Porous Medium, *Journal Porous Media*, *14* (2011), 11, pp. 1007-1018
[10] Eldabe, N. T. M., *et al*., Motion of a Thin Film of a Fourth Grade Nanofluid with Heat Transfer Down a Vertical Cylinder: Homotopy Perturbation Method Application, *Journal Adv. Res. Fluid Mech. Thermal Sci*., *66* (2020), 2, pp. 101-113
[11] Agbaje, T. M., *et al*., A Numerical Study of Unsteady Non-Newtonian Powell-Eyring Nanofluid-Flow over a Shrinking Sheet with Heat Generation and Thermal Radiation, *Alexandria Eng. J*., *56* (2017), 1, pp. 81-91
[12] Abou-Zeid, M. Y., Implicit Homotopy Perturabation Method for MHD Non-Newtonian Nanofluid Flow with Cattaneo-Christov Heat Flux Due to Parallel Rotating Disks, *Journal Nanofluids*, *8* (2019), 8, pp. 1648-1653
[13] Eldabe, N. T. M., Abou-Zeid, M. Y., Radially Varying Magnetic Field Effect on Peristaltic Motion with Heat and Mass Transfer of a Non-Newtonian Fluid between Two Co-Axial Tubes, *Thermal Science*, *22* (2018), 6A, pp. 2069-2080
[14] Eldabe, N. T., *et al*., A Semianalytical Technique for MHD Peristalsis of Pseudoplastic Nanofluid with Temperature-Dependent Viscosity: Application in Drug Delivery System, Heat Transfer – Asian Research, *49* (2020), 1, pp. 2449-2458
[15] Mansour, H. M., Abou-Zeid, M. Y., Heat and Mass Transfer Effect on Non-Newtonian Fluid-Flow in a Non-Uniform Vertical Tube with Peristalsis, *Journal of Advanced Research in Fluid Mechanics and Thermal Sciences*, *61* (2019), 1, pp. 44-62
[16] Eldabe, N. T., *et al*., Electromagnetic Steady Motion of Casson Fluid with Heat and Mass Transfer through Porous Medium Past a Shrinking Surface, *Thermal Science*, *25* (2021), 1, pp. 257-265
[17] Bhatti, M. M., *et al*., Intra-Uterine Particle-Fluid Motion through a Compliant Asymmetric Tapered Channel with Heat Transfer, *Journal Therm. Anal. Calorim*., *144* (2021), Sept., pp. 2259-2267
[18] Eldabe, N. T. M., *et al*., Peristaltic Motion of Non-Newtonian Fluid with Heat and Mass Transfer through a Porous Medium in Channel under Uniform Magnetic Field, *Journal Fluids*, *2014* (2014), ID 525769
[19] Zhang, L., *et al*., Entropy Analysis on the Blood Flow through Anisotropically Tapered Ateries Filled with Magnetic Zinc-Oxide (ZnO) Nanoparticles, *Entropy*, *22* (2020), 10, 1070
[20] Eldabe, N. T., *et al*., The MHD Peristaltic Transport of Bingham Blood Fluid with Heat and Mass Transfer through a Non-Uniform Channel, *Journal of Advanced Research in Fluid Mechanics and Thermal Science*, *77* (2021), 2, pp. 145-159, 2021
[21] Eldabe, N. T. M., *et al*., Wall Properties Effect on the Peristaltic Motion of a Coupled Stress Fluid with Heat and Mass Transfer through a Porous Media, *Journal Eng. Mech*., *142* (2015), 3, 4015102
[22] Rahimi, J., *et al*., Solution of the Boundary-Layer Flow of an Eyring-Powell Non-Newtonian Fluid over a Linear Stretching Sheet by Collocation Method, *Alexandria Eng. J*., *56* (2017), 4, pp. 621-627
[23] Gireesha, B. J., *et al*., Melting Heat Transfer in Boundary-Layer Stagnation-Point Flow of Nanofluid Toward a Stretching Sheet with Induced Magnetic Field, *Eng. Sci. Technol. an Int. J*., *19* (2016), 1, pp. 313-321
[24] Sheikholeslami, M., Rokni, H. B., Nanofluid Two-Phase Model Analysis in the Existence of Induced Magnetic Field, *Int. J. Heat Mass Transf*., *107* (2017), Apr., pp. 288-299
[25] Sheikholeslami, M., *et al*., Influence of Induced Magnetic Field on Free Convection of Nanofluid Considering Koo-Kleinstreuer-Li (KKL) Correlation, *Appl. Sci*., 6 (2016), 11, 324
[26] Mohamed, M. A., Y. Abou-Zeid, Y., The MHD Peristaltic Flow of Micropolar Casson Nanofluid through a Porous Medium between Two Co-Axial Tubes, *Journal Porous Media*, *22* (2019), 9, pp. 1079-1093
[27] Abou-Zeid, M. Y., Homotopy Perturbation Method for Couple Stresses Effect on MHD Peristaltic Flow of a Non-Newtonian Nanofluid, *Microsys. Technol*., *24* (2018), Apr., pp. 4839-4849
[28] Eldabe, N. T., *et al*., Instantaneous Thermal-Diffusion and Diffusion-Thermo Effects on Carreau Nanofluid-Flow over a Stretching Porous Sheet, *Journal of Advanced Research in Fluid Mechanics and Thermal Sciences*, *72* (2020), 2, pp. 142-157
[29] Hayat, T., *et al*., The MHD Flow of Powell-Eyring Nanofluid over a Non-Linear Stretching Sheet with Variable Thickness, *Results Phys*., *7* (2017), Dec., pp. 189-196

[30] Eldabe, N. T., *et al*., The 2-D Boundary-Layer Flow with Heat and Mass Transfer of Magnetohydrodynamic Non-Newtonian Nanofluid through Porous Medium over a Semi-Infinite Moving Plate, *Microsyst. Technol*., 24 (2018), 7, pp. 2919-2928
[31] Abou-Zeid, M. Y., Homotopy Perturbation Method for MHD Non-Newtonian Nanofluid Flow through a Porous Medium in Eccentric Annuli with Peristalsis, *Thermal Scienc*e., *21* (2017), 5, pp. 2069-2080
[32] Ali, F. M., The MHD Stagnation-Point Flow and Heat Transfer Towards Stretching Sheet with an Induced Magnetic Field, *Appl. Math. Mech*., *32* (2011), 4, pp. 409-418
[33] Khan, W. A., Makinde, O. D., The MHD Nanofluid Bioconvection Due to Gyrotactic Microorganisms over a Convectively Heat Stretching Sheet, *Int. J. Therm. Sci*., 81 (2014), 1, pp. 118-124
[34] Eldabe, N. T. M., The MHD Peristaltic Flow of Non-Newtonian Power-Law Nanofluid through a Non-Darcy Porous Medium Inside a Non-Uniform Inclined Channel, *Arch Appl Mech*., *91* (2021), Oct., pp. 1067-1077
[35] Waqas, M., *et al*., Transport of Magnetohydrodynamic Nanomaterial in a Stratified Medium Considering Gyrotactic Microorganisms, *Phys. B Condens. Matter*, *529* (2018), Oct., pp. 33-40
[36] Abou-Zeid, M. Y., Homotopy Perturbation Method to Gliding Motion of Bacteria on a Layer of Power-Law Nanoslime with Heat Transfer, *Journal Comput. Theor. Nanosci*., *12* (2015), 10, pp. 3605-3614
[37] Zaffar, , M., Iqbal, Z., Interaction of Induced Magnetic Field and Stagnation Point Flow on Bioconvection Nanofluid Submerged in Gyrotactic Microorganisms, *Journal Mol. Liq*., *224* (2016), Dec., pp. 1083-1091
[38] Bhatti, M. M., *et al*., Simultaneous Effects of Coagulation and Variable Magnetic Field on Peristaltically Induced Motion of Jeffrey Nanofluid Containing Gyrotactic Microorganism, *Microvasc. Res*., *110* (2017), Mar., pp. 32-42
[39] Ibrahim, W., The Effect of the Induced Magnetic Field and Convective Boundary Condition on MHD Stagnation Point Flow and Heat Transfer of Upper-Convected Maxwell Fluid in the Presence of Nanoparticle Past a Stretching Sheet, *Propuls. Power Res*., *5* (2015), 2, pp. 164-175

Paper submitted: April 8, 2020
Paper revised: April 28, 2021
Paper accepted: May 5, 2021